

# S-wave quantum entanglement in a harmonic trap

Jia Wang, C. K. Law and M.-C. Chu

*Department of Physics, The Chinese University of Hong Kong, Shatin, Hong Kong SAR, China*

(Dated: May 24, 2019)

We analyze the quantum entanglement between two interacting atoms trapped in a spherical harmonic potential. At ultra-cold temperature, ground state entanglement is generated by the dominated s-wave interaction. Based on a regularized pseudo-potential Hamiltonian, we examine the quantum entanglement by performing the Schmidt decomposition of low-energy eigenfunctions. We indicate how the atoms are paired and quantify the entanglement as a function of a modified s-wave scattering length inside the trap.

PACS numbers: 03.67.Mn 03.65.Ud

The interactions between trapped ultra-cold atoms govern many interesting collective quantum phenomena, ranging from Bose-Einstein condensation [1] to recently observed fermion superfluid [2]. At sufficiently low energies, it is known that short ranged atom-atom interactions can be replaced by a pointlike regularized pseudo-potential under the shape independent approximation [3]. The strength of such a pseudo-potential is determined by a s-wave scattering length  $a$  only, and hence one can control atom-atom interaction by tuning the scattering length via the technique of Feshbach resonance. For trapped systems, the theory of pseudo-potential has been examined in details by several authors [4, 5]. As long as the range of the actual atom-atom interaction is short compared with the width of the trap, low energy eigenfunctions can be accurately captured by the eigenfunctions of the pseudo-potential, except for a few tightly bound states that may exist inside the range of the inter-atomic potential. Such a universal applicability is the essence of shape independent approximation. Therefore the study of eigenfunctions of pseudo-potentials would provide useful insight about generic features of two-body correlations in the low energy regime.

In this paper, we address the interesting question of how the scattering length controls quantum correlations between two ultra-cold atoms inside a harmonic trap. Specifically, we will examine quantum entanglement arising from the s-wave interaction described by a regularized pseudo-potential. Unlike free space scattering problems [6, 7], the harmonic trap provides a spatial confinement of the two particles. Such a confinement modifies the scattering length [5] and most importantly, the structure of entanglement associated with the atom's continuous degrees of freedom. By performing the Schmidt decomposition of low energy eigenfunctions, we show that quantum entanglement is manifested as pairing of atoms in a set of orthogonal mode functions in three-dimensional space. In particular, the angular momenta are identified as good quantum numbers to characterize the Schmidt mode functions. Our main purpose of this paper is to quantify the degree of entanglement as a function of s-wave scattering length  $a$ . As we shall see below, the entanglement is sensitive to the values of  $a$  when  $a$  exceeds the width of the non-interacting ground state wave function. A particularly interesting situation is the large scattering length limit:  $|a| \rightarrow \infty$ , in which we find that the energy eigenfunctions have closed analytic forms. We will discuss the nature of quantum entanglement in this limit.

To begin with, we consider a system of two interacting atoms with equal mass trapped in a spherical harmonic potential. The Hamiltonian of the system is given by,

$$H = -\frac{\hbar^2}{2m}\nabla_1^2 - \frac{\hbar^2}{2m}\nabla_2^2 + \frac{1}{2}m\omega^2r_1^2 + \frac{1}{2}m\omega^2r_2^2 + V(\mathbf{r}_1 - \mathbf{r}_2), \quad (1)$$

where  $\mathbf{r}_1$  and  $\mathbf{r}_2$  are the position vectors of the two atoms,  $m$  is the mass of the atom, and  $\omega$  is the trap frequency. The interaction between the two atoms is described by the short range potential  $V$  which will be replaced by a pseudo-potential (see Eq. 3) under the shape independent approximation. For convenience, we separate the Hamiltonian into a center-of-mass part and a relative part,  $H = H_{cm} + H_{rel}$  so that

$$H_{cm} = -\frac{1}{8}\nabla_R^2 + 2R^2, \quad (2)$$

$$H_{rel} = -\frac{1}{2}\nabla_r^2 + \frac{1}{2}r^2 + 2\pi a\delta^{(3)}(\mathbf{r})\frac{\partial}{\partial r}r, \quad (3)$$

with  $\mathbf{R} = (\mathbf{r}_1 + \mathbf{r}_2)/2$  and  $\mathbf{r} = \mathbf{r}_1 - \mathbf{r}_2$ . Here the energy and length are expressed in units of  $\hbar\omega$  and  $(\hbar/\mu\omega)^{1/2}$  (where  $\mu = m/2$  is the reduced mass) respectively. The strength of the pseudo-potential is characterized by the modified s-wave scattering length  $a$ . For a given inter-atomic potential, the precise value of  $a$  depends on the trapping potential and it can be determined self-consistently by the methods discussed in Ref. [5]. In this paper we will treat  $a$  as a parameter of the Hamiltonian.

The s-wave eigen-functions of the  $H$  have been solved analytically in Ref. [4]. Given a scattering length, the eigen-energy  $E$  of  $H_{rel}$  is defined by the solution of:

$$\frac{\Gamma(-E/2 - 1/4)}{2\Gamma(-E/2 + 3/4)} = a \quad (4)$$

with  $\Gamma$  being the gamma function. The eigenfunctions of  $H_{rel}$  with the energy  $E$  are given by:

$$\psi_E(\mathbf{r}) = Ae^{-r^2/2}U(-E/2 + 3/4, 3/2, r^2) \quad (5)$$

where  $A$  is a normalization constant, and  $U(\alpha, \beta, z)$  is the Kummer's function [10].

In this paper we assume that the center of mass wave function is the ground state of  $H_{cm}$ , which is a simple gaussian:  $\Phi(\mathbf{R}) = 2\sqrt{2}e^{-2R^2}/\pi^{3/4}$ . Combining  $\Phi(\mathbf{R})$  with  $\psi_E(\mathbf{r})$ , the two-particle energy eigenfunctions are given by

$$\Psi(\mathbf{r}_1, \mathbf{r}_2) = \Phi(\mathbf{R})\psi_E(\mathbf{r}). \quad (6)$$

In Fig. 1, we illustrate how the eigen-energies depend on the scattering length. For convenience, we choose to plot with the inverse of scattering length, i.e.,  $1/a$ , in order to indicate the continuous branch associated with the ground states. It should be noted that the ground state energy becomes large and negative when  $1/a$  is positive and large. This feature also occurs in the absence of the harmonic trapping potential, and it is due to the existence of a tightly bound state in the  $a \rightarrow 0^+$  limit [4]. As an illustration, the radial probability density of the ground state at several values of  $a$  are plotted in Fig. 2.

The characterization of quantum entanglement is achieved by Schmidt decomposition of  $\Psi(\mathbf{r}_1, \mathbf{r}_2)$ , which reads:

$$\Psi(\mathbf{r}_1, \mathbf{r}_2) = \sum_j \sqrt{\lambda_j} u_j(\mathbf{r}_1) v_j(\mathbf{r}_2), \quad (7)$$

where  $\lambda_j$  are eigenvalues, and  $u_j$  and  $v_j$  are Schmidt eigenmodes defined by,

$$\int d\mathbf{r}'_1 \int d\mathbf{r}_2 \Psi(\mathbf{r}_1, \mathbf{r}_2) \Psi^*(\mathbf{r}'_1, \mathbf{r}_2) u_j(\mathbf{r}'_1) = \lambda_j u_j(\mathbf{r}_1), \quad (8)$$

$$\int d\mathbf{r}'_2 \int d\mathbf{r}_1 \Psi(\mathbf{r}_1, \mathbf{r}_2) \Psi^*(\mathbf{r}_1, \mathbf{r}'_2) v_j(\mathbf{r}'_2) = \lambda_j v_j(\mathbf{r}_2). \quad (9)$$

Note that the mode functions  $u_j$  form a complete and orthonormal set, and the same is true for  $v_j$ . If the atom 1 appears in the mode  $u_j$ , then with certainty the atom 2 must be in the mode  $v_j$ . In other words, Eq. (7) indicates the pairing structure of the two particle state. In addition, the distribution of  $\lambda_j$  provides a measure of the degree of entanglement. This is usually discussed in terms of the entanglement entropy  $S = -\sum_j \lambda_j \log \lambda_j$ . However, a more transparent measure is the effective number of Schmidt modes, which is provided by the Schmidt number:  $K \equiv 1/\sum_j \lambda_j^2$  [8]. A disentangled (product) state corresponds to  $K = 1$ , i.e., there is only one term in the Schmidt decomposition. The larger the value of  $K$ , the higher the entanglement. We point out that  $1/K$  equals the purity of the density matrix of an individual particle. The purity has also been employed as a measure of the degree of entanglement in various physical situations [6, 9].

To carry out the Schmidt decomposition of the wave functions in three dimension, we note that  $R = \sqrt{r_1^2 + r_2^2 + 2r_1 r_2 \cos \gamma}/2$  and  $r = \sqrt{r_1^2 + r_2^2 - 2r_1 r_2 \cos \gamma}$ , where  $\gamma$  is the angle between  $\mathbf{r}_1$  and  $\mathbf{r}_2$ . Therefore the wave function  $\Psi(\mathbf{r}_1, \mathbf{r}_2) = \Psi(r_1, r_2, \cos \gamma) = \sum_{l=0}^{\infty} \alpha_l(r_1, r_2) P_l(\cos \gamma)$ , where  $P_l(x)$  is the Legendre polynominal, and

$$\alpha_l(r_1, r_2) = \frac{2l+1}{2} \int_0^\pi d\gamma \sin \gamma \cdot \Psi(r_1, r_2, \cos \gamma) P_l(\cos \gamma). \quad (10)$$

With the help of the addition formula:  $(2l+1)P_l(\cos \gamma) = 4\pi \sum_{m=-l}^l Y_{l-m}(\theta_1, \phi_1) Y_{lm}(\theta_2, \phi_2)$ , we have

$$\Psi(\mathbf{r}_1, \mathbf{r}_2) = 4\pi \sum_{l=0}^{\infty} \sum_{m=-l}^l \frac{\alpha_l(r_1, r_2)}{2l+1} Y_{l-m}(\theta_1, \phi_1) Y_{lm}(\theta_2, \phi_2). \quad (11)$$

This expression is already partially in the Schmidt form, because the pairing of angular functions has been identified. The remaining task is to decompose  $\alpha_l(r_1, r_2)$  for each  $l$ . This can be achieved by performing the Schmidt decomposition of the function  $r_1 r_2 \alpha_l(r_1, r_2)$ , i.e.,

$$r_1 r_2 \alpha_l(r_1, r_2) = \sum_n \sqrt{\lambda_{nl}} u_{nl}(r_1) v_{nl}(r_2). \quad (12)$$

Here the prefactor  $r_1 r_2$  is introduced in order to ensure correct normalization in radial directions. The fact that the angular parts of Schmidt modes can be obtained analytically reduces the computational difficulty in the original three-dimensional problem. Finding  $u_{nl}$ ,  $v_{nl}$  and  $\lambda_{nl}$  in Eq. (12) is a relatively simple numerical task, because  $r_1 r_2 \alpha_l(r_1, r_2)$  behaves as a two-particle (one dimensional) wave function in non-negative  $r_1$  and  $r_2$  regions. We have solved  $u_{nl}$ ,  $v_{nl}$  and  $\lambda_{nl}$  numerically for a range of  $l$ . Because of the symmetry properties of  $r_1 r_2 \alpha_l(r_1, r_2)$ ,  $u_{nl}$  and  $v_{nl}$  are the same. For low energy states considered in this paper,  $l$  up to 20 are typically sufficient in order to obtain convergent results.

The final form of the Schmidt decomposition of the wave function Eq. (5) now reads:

$$\Psi(\mathbf{r}_1, \mathbf{r}_2) = \sum_{n=1}^{\infty} \sum_{l=0}^{\infty} \sum_{m=-l}^l \left( \frac{4\pi\sqrt{\lambda_{nl}}}{2l+1} \right) \left[ \frac{u_{nl}(r_1)}{r_1} Y_{l-m}(\theta_1, \phi_1) \right] \left[ \frac{v_{nl}(r_2)}{r_2} Y_{lm}(\theta_2, \phi_2) \right]. \quad (13)$$

Our derivation indicates a general feature that for any wave function that is a function of distances  $R$  and  $r$  only, the angular parts of Schmidt modes are simply the spherical harmonics. The pairing involves angular momentum quantum numbers  $(l, m)$  and  $(l, -m)$ , i.e., the same  $l$  and opposite  $m$  must be paired. In addition, each  $m$  is of equal weight for a given  $l$ . Therefore if one could select Schmidt modes with a fixed  $n$  and  $l$  via projective measurement, then the resulting state is a maximally entangled state among various  $m$ 's on the projected  $l$  manifold.

The value of  $K$  associated with the state (13) is given by,

$$K = 1 / \sum_{n=1}^{\infty} \sum_{l=0}^{\infty} \Lambda_{nl}^2 \quad (14)$$

where  $\Lambda_{nl} = 16\pi^2 \lambda_{nl} / (2l+1)^{3/2}$  is defined. In Fig. 3 we plot the values of  $K$  as a function of the inverse of the scaled scattering length for low energy states. We notice that higher excited states generally have higher quantum entanglement. However, the ground state shows a distinct behavior in the positive  $1/a$  region, where we notice a shape rise of  $K$  as  $1/a$  increases. The strong entanglement is understood as the appearance of increasingly bounded atoms implied in the ground state energy curve in Fig. 1 (see also a typical wave function in Fig. 2). Our numerical calculations indicate an empirical relation for the ground state:  $K \approx 1.86e^{0.82/a}$  for  $0 < 1/a < 2$ , which is an exponential dependence. We remark that the large  $1/a$  limit has to be examined carefully, because the shape independent approximation would become invalid if a significantly portion of the wave function is inside the range of the actual atom-atom potential.

An interesting feature observed in Fig. 3 is that quantum entanglement is only sensitive to a range of scaled scattering lengths (with the exception of the ground state in the  $1/a > 0$  region). Such a window of scaled scattering lengths is highlighted by dashed lines in Fig. 3, where we found that  $K$  changes significantly with  $1/a$  when  $1/|a| < 2$ . Recalling that we are using the length unit defined by the harmonic trap, our results suggest that the s-wave interaction can appreciably affect quantum entanglement when  $a$  is greater than or comparable with the width of a ground state particle inside the trap, i.e.,  $|a| > (\hbar/2m\omega)^{1/2}$ .

The limit of  $|a| \rightarrow \infty$  or  $1/|a| \rightarrow 0$  is located at the center of the entanglement sensitive window mentioned above. In such a limit, we find that the eigenfunctions take simple analytic forms. We present some of the low energy eigenfunctions of  $H$  in the limit  $|a| \rightarrow \infty$ :

$$\Psi_{10}(\mathbf{r}_1, \mathbf{r}_2) = \frac{2}{\pi^{3/2}} \frac{e^{-r_1^2} e^{-r_2^2}}{|\mathbf{r}_1 - \mathbf{r}_2|}, \quad (15)$$

$$\Psi_{11}(\mathbf{r}_1, \mathbf{r}_2) = \frac{\sqrt{2}}{\pi^{3/2}} \frac{e^{-r_1^2} e^{-r_2^2}}{|\mathbf{r}_1 - \mathbf{r}_2|} \left[ 1 - (\mathbf{r}_1 - \mathbf{r}_2)^2 \right], \quad (16)$$

$$\Psi_{12}(\mathbf{r}_1, \mathbf{r}_2) = \frac{\sqrt{3/2}}{\pi^{3/2}} \frac{e^{-r_1^2} e^{-r_2^2}}{|\mathbf{r}_1 - \mathbf{r}_2|} \left[ 1 - 4(\mathbf{r}_1 - \mathbf{r}_2)^2 + \frac{4}{3}(\mathbf{r}_1 - \mathbf{r}_2)^4 \right]. \quad (17)$$

Here Eqs. (15-17) correspond to the energy eigenfunctions (center of mass + relative coordinates) associated with the lowest three states of  $H_{rel}$ , and the ground state of  $H_{cm}$ . We remark that the regularized pseudo-potential method can only describe wave functions at inter-atomic distance much larger than the range of the actual inter-atomic potential

$b$ , i.e.,  $|\mathbf{r}_1 - \mathbf{r}_2| \gg b$ . Inside the interaction range  $b$ , the actual wave functions remain finite as  $|\mathbf{r}_1 - \mathbf{r}_2| \rightarrow 0$ . Therefore the singular behavior at  $\mathbf{r}_1 = \mathbf{r}_2$  in Eqs. (15-17) is only an artifact of the shape independent approximation, and hence these wave functions should be understood for  $|\mathbf{r}_1 - \mathbf{r}_2| \gg b$  only. However, since  $b$  is typically much smaller than  $(\hbar/\mu\omega)^{1/2}$  (which is about the width of  $\Psi$ ), the probability of finding the two particles within the range  $b$  is negligible [11]. This justifies the use of the shape independent approximation here. For the wave functions given in Eqs. (15-17), the corresponding  $K$  values are 1.98, 3.45, and 9.11 respectively.

The structure of quantum entanglement in the  $|a| \rightarrow \infty$  limit can be made apparent by studying the distribution of Schmidt eigenvalues. Since Schmidt modes with the same  $l$  but different  $m$ 's have equal weight, we need to consider discrete probability distribution  $\Lambda_{nl}$  only. In Fig. 4, we display the distribution for  $\Psi_{10}$  and  $\Psi_{11}$ . We see that the distributions concentrate mostly on the  $n = 1$  manifold. This indicates that the quantum entanglement between the two particles are mainly manifested in the angular variables. For the ground state wave function  $\Psi_{10}$ , the entanglement  $K \approx 2$  is not high because of the presence of a dominant  $(n, l, m) = (1, 0, 0)$  Schmidt mode, which covers about 70% probability of the state (Fig. 4a). For the first excited state  $\Psi_{11}$ , the significance of angular correlations is more apparent as shown in Fig. 4b.

To summarize, we present a procedure to analyze the s-wave quantum entanglement between two ultra-cold atoms in a spherical harmonic trap. The s-wave interaction is captured by the regularized pseudo-potential. By performing the Schmidt decomposition of low energy eigenstates, we quantify the quantum entanglement and indicate its dependence on the modified scattering length. In particular, our Schmidt analysis reveals the angular correlations by showing explicitly the pairing of spherical harmonic functions. For small and positive  $a$ , the ground states are highly entangled states, and we explain this feature as a consequence of tight binding between the atoms. For low excited states, we find that the atom-atom interaction can only appreciably affect the entanglement when the scattering length is larger than the width of the (non-interacting) ground state defined by the trap. However, the degree of entanglement remains finite in the large scattering length limit. Our work here indicates that quantum entanglement can be controlled by the scattering length. Conversely, one could also deduce the value of scattering length by ‘measuring’ the degree of quantum entanglement. To explore the full applications of s-wave quantum entanglement would require measurement schemes for  $K$ , and this is a challenging open topic for further investigations.

### Acknowledgments

The authors thank Stephen K. Y. Ho for discussions. This work is supported in part by the Research Grants Council of the Hong Kong Special Administrative Region, China (Project No. 400504).

---

[1] For a review see, Anthony J. Leggett, Rev. Mod. Phys. **73**, (2001).  
 [2] For an overview see, T. L. Ho, Science, **305**, 1114 (2004).  
 [3] K. Huang, *Statistical Mechanics* (Wiley, New York 1987).  
 [4] T. Busch, B. G. Englert, K. Rzazewski, and M. Wilkens, Found. Phys. **28**, 549 (1998).  
 [5] M. Block and M. Holthaus, Phys. Rev. A **65**, 052102 (2002); E. Tiesinga, C. J. Williams, F. H. Mies, and P. S. Julienne, Phys. Rev. A **61**, 063416 (2000); E. L. Bolda, E. Tiesinga, and P. S. Julienne, Phys. Rev. A **66**, 013403 (2002).  
 [6] C. K. Law, Phys. Rev. A **70**, 062311 (2004).  
 [7] A. Tal and G. Kurizki (private communications).  
 [8] R. Grobe, K. Rzazewski and J. H. Eberly, J. Phys. B **27**, L503 (1994); W.-C. Liu, J. H. Eberly, S. L. Haan and R. Grobe, Phys. Rev. Lett. **83**, 520 (1999); R. E. Wagner, P. J. Peverly, Q. Su, and R. Grobe, Laser Phys. **11**, 221 (2001); C. K. Law and J. H. Eberly, Phys. Rev. Lett. **92**, 127903 (2004); P. Krekora, Q. Su, and R. Grobe, J. Mod. Opt. **52**, 489 (2005).  
 [9] Ph. Jacquod, Phys. Rev. Lett. **92**, 150403 (2004).  
 [10] M. Abramowitz and I. A. Stegun, eds., *Handbook of Mathematical Functions* (Dover, New York, 1972).  
 [11] For example, the lowest order van der Waals interaction has a characteristic range of the order of 50 Å, and the width of typical trap of frequency 100 Hz is of order 1 μm.

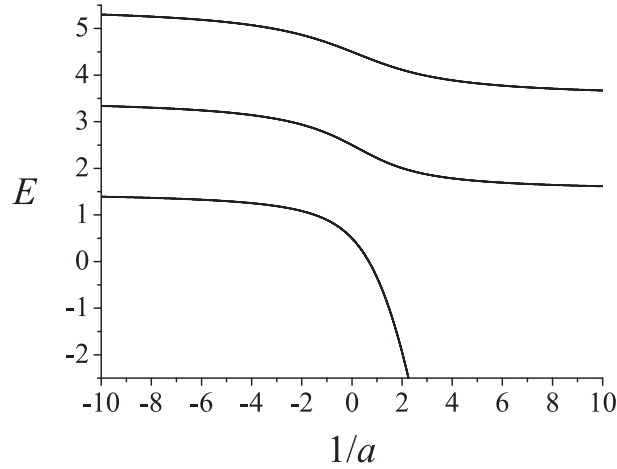


FIG. 1: Eigen-energies of  $H_{rel}$  as a function of the inverse of (dimensionless) scaled scattering length.  $E$  is in units of  $\hbar\omega$ . The three curves correspond to the lowest three states with zero angular momentum (in relative coordinate).

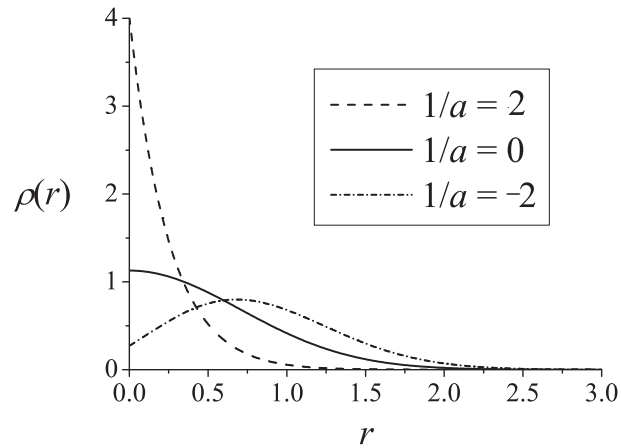


FIG. 2: Radial densities  $\rho(r) \equiv 4\pi r^2 |\psi_E(r)|^2$  associated with the ground state wave functions at  $1/a = 0, \pm 2$ .

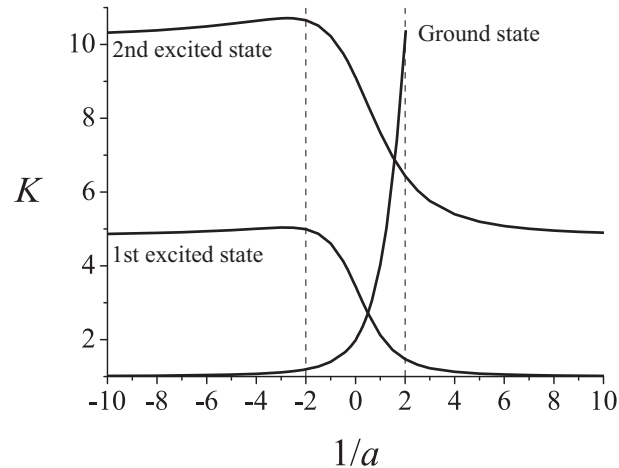


FIG. 3: Schmidt number as a function of the inverse of (dimensionless) scaled scattering length for the lowest three eigenstates of  $H_{rel}$  with zero angular momentum in the relative coordinate.

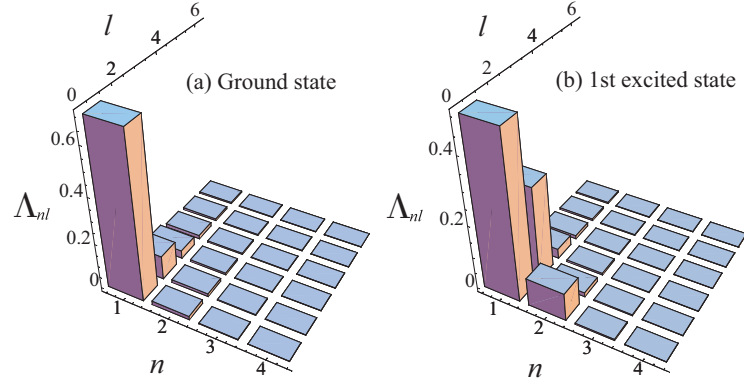


FIG. 4: Distribution of  $\Lambda_{nl}$  (see text) at  $1/a = 0$  for: (a) ground state and (b) the first excited state.